CrystEngComm

Accepted Manuscript

ROYAL SOCIETY OF CHEMISTRY

www.rsc.org/crystengcomm

Cite this: DOI: 10.1039/c0xx00000x

www.rsc.org/xxxxxx

ARTICLE TYPE

Supramolecular features in the engineering of 3d metal complexes with phenyl-substituted imidazoles as ligands: the case of copper(II)

Konstantina A. Kounavi,[a] Alexandros A. Kitos,[a] Eleni E. Moushi,[b] Manolis J. Manos,[‡b] Constantina Papatriantafyllopoulou,[b] Anastasios J. Tasiopoulos,[b] Spyros P. Perlepes[a] and Vassilios Nastopoulos*[a]

Received (in XXX, XXX) Xth XXXXXXXXX 20XX, Accepted Xth XXXXXXXXX 20XX
DOI: 10.1039/b000000x

With the aim of recording and assessing the role and impact of the various non-covalent interactions activated during the self-assembly process of 3d metal complexes with organic ligands, the synthesis and X-ray characterization of a series of eleven Cu(II) complexes with two phenyl-substituted imidazoles [1-methyl-4,5-diphenylimidazole (L) and 4,5-diphenylimidazole (HL′)] as ligands have been carried out. A variety of parameters and conditions have been probed using the general Cu^{II}/X^{-}/L or HL′ (X^{-} = Cl^{-}, Br^{-}, I^{-}, NO_3^{-}, NO_2^{-}, ClO_4^{-}) reaction system. In structures with the ligand L (**1**–**7**), lacking any group capable of establishing strong intermolecular H-bonding contacts, the burden of the supramolecular organization is undertaken by weak, yet productive, C–H···X and C–H···π interactions, while the metal ions keep their preferred coordination geometries (square planar and square pyramidal). In compounds with the ligand HL′ (**8**–**11**), however, robust and recurring N–H···X (X = Cl or O) motifs have the leading role towards effectively directing the self-assembly; flexible water molecules contribute actively, when needed $\{[Cu(HL')_4](ClO_4)_2 \cdot EtOH \cdot CH_2Cl_2 \cdot H_2O\}$, to maximize the number of these motifs. At a second level of organization, additional subordinate C–H···Cl or O and C–H···π interactions, complement the rigidity of the structures. The distortion of the coordination environment (seesaw) of Cu^{II} centres in compounds $[CuCl_2(HL')_2] \cdot Me_2CO \cdot 0.25H_2O$ and $[CuCl(HL')_3]Cl \cdot 0.6H_2O$ appears to reflect the balance of forces within the crystallization system to facilitate the necessary orientation of the tectons so as to form the hierarchically prevailing N–H···X synthons. Moreover, the small number of intermolecular π···π contacts observed, despite the abundance of aromatic rings, indicates their weakness to form at the expenses of stronger interactions. Lastly, comparison with previously structurally characterized analogous Co(II), Ni(II) and Zn(II) complexes (*vide infra*) corroborates and adds confidence to the conclusions deduced herein.

Introduction

The structural chemistry of organic or metal-based architectures (discrete or polymeric) continues to attract the interest of scientists in Crystal Engineering, mainly due to the development of new phenomena and the potential applications of the resultant materials.[1-3] In metallosupramolecular chemistry, in addition to the coordination bond, hydrogen bonds are effective in establishing particular contacts which occur regularly, and play a significant and repetitive role in directing molecules during crystallization.[4]

We have recently explored the supramolecular architectures of a series of Co(II), Zn(II) and Ni(II) complexes with phenyl-substituted imidazole ligands,[5,6] which have demonstrated the distinct role of the hydrogen-bond motifs to direct the self-assembly along the structures in spite of the variation of their crystalline environments. In this regard, it seemed interesting to accomplish a study by exploiting a metal known for its variety in coordination geometries, namely Cu(II).

Copper(II) is a special metal ion in coordination chemistry[7] and it has been named 'chameleon'.[8] The $3d^9$ configuration makes Cu^{II} subject to Jahn-Teller distortion if placed in an environment of cubic (*i.e.* regular octahedral or tetrahedral) symmetry, and this has a profound effect on all its stereochemistry. Thus, distorted octahedral, tetrahedral, square pyramidal and trigonal bipyramidal, as well as square planar coordination geometries dominate the coordination chemistry of copper(II). These special features of Cu^{II} are expected to alter its metallosupramolecular chemistry.

We have therefore designed and prepared a series of Cu(II) complexes with the monodentate ligands 1-methyl-4,5-

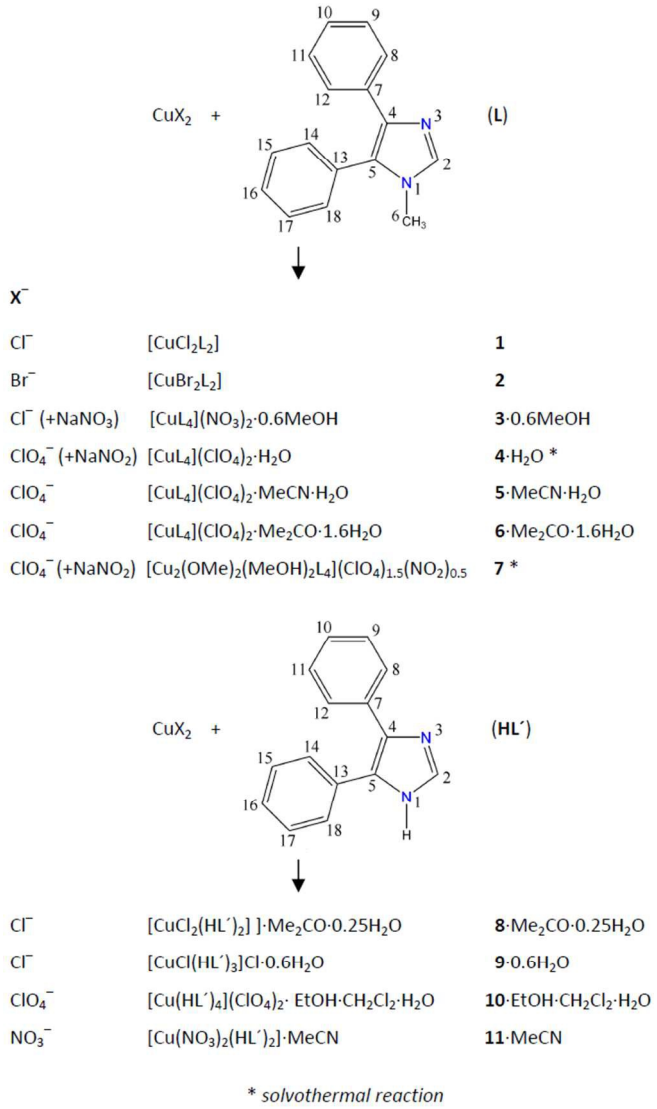

Scheme 1 Structural formulae of the free ligands L and HL′, and the crystallographically determined formulae and numbering scheme of their Cu(II) complexes.

diphenylimidazole (L) and 4,5-diphenylimidazole (HL′), coordinated to the metal ion *via* their pyridine-type N3 atom (Scheme 1). We opted for these ligands because (i) ligand HL′, in contrast to L, has a hydrogen-bond donor (the pyrrolic-type N1 atom) enabling the formation of motifs that can potentially assist the molecular self-assembly, (ii) they are both capable of π···π stackings through their phenyl rings and the 5-membered heterocyclic ring; these interactions can play a notable role in defining structures which lack strong hydrogen bond donors (as in complexes with L), (iii) they have similar molecular structures and therefore comparative studies can be more convenient and convincing, and (iv) we wanted to compare the current compounds with the respective of Co(II), Zn(II) and Ni(II) reported by our group previously.[5,6] There are relatively few reports on the coordination chemistry of phenyl-substituted imidazoles, and especially about ligands L[5,6,9,10] and HL′.[6,11] The choice of the ions X^- (X^- = Cl^-, Br^-, I^-, NO_3^-, NO_2^-, ClO_4^-) used was based on (i) their tendency to coordinate terminally as monodentate or bidentate ligands,[5,6] thereby excluding the possibility of coordination polymers, (ii) their ability to act as counterions;[6,12] thus cationic complexes would also be expected, offering the opportunity to study the role of the charged counterions in the self-assembly process, and (iii) their size[13] and shape, in order to study their effect on the coordination geometry of the metal and the subsequent complex stoichiometry (when coordinated), or their spatial role in the motif formation and packing organization (as counterions). A total of eleven new Cu(II) complexes of L and HL′ are reported herein, prepared and characterized in line of this approach. One synthetic or crystallization parameter at a time was varied during each set of experiments so as to assess its relative effect on the product identity.

Results and Discussion

Synthetic comments

With a desire to prepare the largest possible number of Cu(II) complexes of L and HL′, a variety of reactions and conditions have been systematically probed (*vide supra*). In some cases triethyl orthoformate (TEOF) was added as a drying agent. The general synthetic route together with the individual formulae of the complexes are illustrated in Scheme 1. Due to the weak coordinating capability of the perchlorate ion, reactions with $Cu(ClO_4)_2·6H_2O$ led to cationic complexes, either mononuclear with an 1:4 Cu^{II}:ligand stoichiometry (**4**–**6**, **10**) or dinuclear with an 1:2 stoichiometry (**7**). Reducing the concentration of reactants and the temperature of the solvothermal reaction used to obtain complex **4** resulted in the formation of the 5-coordinate dinuclear compound **7**. Surprisingly, variation in the crystallization temperature for complex **8** (21 °C) yielded complex **9** (5 °C) with a different stoichiometry. Basic counterions, *e.g.* $MeCO_2^-$ ions, gave evidence of ligand deprotonation in the case of HL′ and formation of polymeric species, which could not be crystallized. It was not possible to isolate any compound containing I^- and NO_2^- ions, either coordinated or as counterions, with the exception of compound **7** which exhibits substitutional disorder of the ClO_4^-/NO_2^- (0.75/0.25) counterions. All crystalline products were characterized by IR spectroscopy, microanalyses, and single-crystal X-ray diffraction.

Description of the structures of complexes 1, 2, 8, and 9

Note: To facilitate discussion, molecular comparison and overlay, the same numbering scheme has been adopted (where applicable) to the ligand atoms (Scheme 1), the coordinated ions, and the counterions/solvents for all compounds presented herein.

This group comprises complexes of the type Cu^{II}/X^-/(L or HL′) with X^- = Cl^- or Br^-. The structures of **1** and **2** (a) have the same space group and quite similar cell dimensions, and (b) the types and the positions of atoms in both structures are the same except for a replacement of the two coordinated chlorine atoms in **1** with bromines in **2**; they are thus isomorphous. The metal centre has a square planar N_2X_2 coordination involving a pyridine-type nitrogen donor atom from each ligand and two terminal halogen atoms (Fig. 1 for complex **2**). Complex **2** is centrosymmetric with

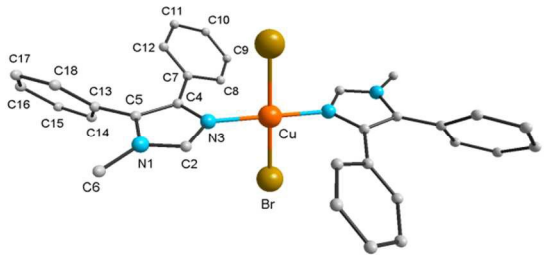

Fig. 1 Molecular structure of complex **2**. The non-labelled atoms are generated by inversion about a centre of symmetry on the copper site. The N3–Cu–Br angle is 89.83(16)º. H-atoms are not shown.

the Cu^{II} located on an inversion centre so as to accommodate the two ligands and the two halogeno atoms in a *trans* disposition, respectively. Due to the planarity of the CuN_2X_2 group imposed by this centre, the value of the τ_4 parameter is 0.00 (as formulated by Hauser & coworkers[14] for the geometry of four-coordinate complexes). Nevertheless, Cu^{II} does not have a perfectly *square* geometry due to a slight deviation from D_{4h} (4/*mmm*) symmetry in its coordination environment, as evidenced by the N–Cu–X values (not exactly 90º) of the CuN_2X_2 group (Fig. 1). The packing organization of **1** and **2** is the same, with the structure of **2** being slightly 'expanded', due to the larger ionic radius of bromides relative to chlorides. In the absence of groups capable of establishing strong H-bonding, the molecules are assembled solely by a combination of weak C–H···X and edge-to-face C–H···π intermolecular interactions[15] connecting them in layers parallel to the (110) plane (Fig. 2 for complex **2** and Table S1, ESI†).

In complexes **8** and **9**, the N1–CH_3 group of ligand L has been deliberately replaced by a N1–H donor group to exploit the impact of its strength and directionality on the self-assembly of the complexes. Complex **8** (Fig. 3) is the analogue of **1**; however, its asymmetric unit includes two unique molecules A and B forming an approximate enantiomeric pair; the conformation of A and that of the inverted B are similar with an overlay rmsd of 0.150 Å. The distorted N_2Cl_2 coordination environment of Cu^{II}

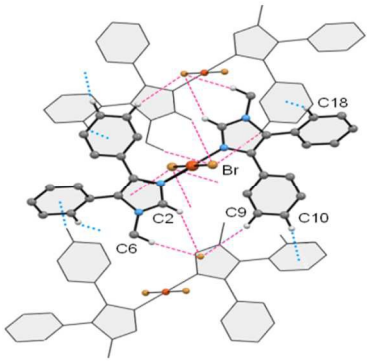

Fig. 2 Supramolecular network in compound **2** generated by C–H···Br (red dashed lines) and C–H···π interactions (blue dotted lines). Each bromide atom acts as a multihydrogen-bonded acceptor. Only the H-atoms involved in these interactions are shown.

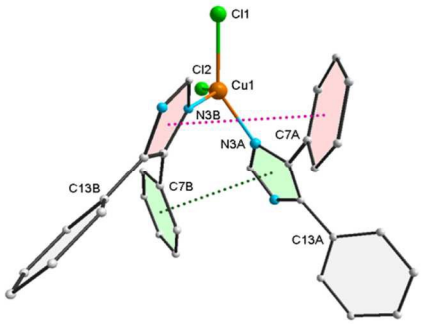

Fig. 3 The structure of molecule A of complex **8** with the two intramolecular π···π motifs: $d_{\pi\cdots\pi}$ = 3.591(2) Å, centroid offset = 1.054(6) Å for the pink pair; $d_{\pi\cdots\pi}$ = 3.722(2) Å, centroid offset = 1.080(5) Å for the green pair. The Cl1–Cu1–N3A angle forms the plank and the Cl2–Cu1–N3B angle the pivot of the seesaw coordination geometry of Cu^{II}. H-atoms are not shown.

has a τ_4 parameter value of 0.52 and 0.53 for molecules A and B, respectively, and, based on the symmetry of the CuN_2Cl_2 group, this can be better described as a seesaw with C_{2v} (*mm*2) symmetry rather than as a distorted tetrahedral one with approximately T_d ($\bar{4}$3m) symmetry. The two ligands of the complex are mutually arranged in a *syn* fashion in an antiparallel way with their NH groups pointing at opposite directions. This arrangement favors the formation of two intramolecular π···π stacking interactions providing stability to the complex. Similar π···π motifs have also been encountered in previously characterized complexes bearing the 4,5-diphenylimidazole moiety,[5,6,10,16] supporting the suitability of L and HL′ as crystal engineering tools. Complex **9** (Fig. 4) is a rather unexpected product in terms of stoichiometry comprising three $[CuCl(HL'_3)]^+$ cations (A, B and C) in its asymmetric unit ($Z' = 3$). The coordination geometry of Cu^{II} is described as a seesaw with a τ_4 parameter value of 0.23, 0.41 and 0.35 for A, B and C, respectively. As in complex **8**, two HL′ ligands in each cation are involved in intramolecular π···π motifs. However, cations A, B and C have significant conformational differences, especially in the orientation of the ligands not involved in intramolecular π···π interactions, presumably to facilitate the self-assembly process (vide *infra*).

At the supramolecular level, the presence of the NH groups together with coordinated/counterion Cl^- species and solvent molecules increase the potential for formation of strong hydrogen-bonded motifs and hence the system complexity. Indeed, the A and B molecules of **8** are linked directly to each other *via* strong N–H···Cl hydrogen bonding towards a 3D assembly (Fig. S1 and Table 1). The water and acetone molecules participate with O_{water}–H···Cl (to molecule A) and N–H···$O_{acetone}$ (to molecule B) bonds, and the packing is further supported *via* weak intermolecular C–H···Cl and C–H···π contacts. There are no intermolecular π···π stackings, despite the freedom allowed to the independent molecules A and B to orient themselves in space, implying the tendency of the system to facilitate the optimization of the dominant N–H···Cl motifs in the crystal.

The leading role of these motifs in the self-assembly process is nicely illustrated in complex **9** (crystallized at lower temperature).

Table 1 Geometry (Å, º) of the strong hydrogen-bonding motifs in compounds **8**–**11**[a]

D–H···A	D–H	H···A	D···A	<(DHA)
8·Me$_2$CO·0.25H$_2$O				
N1A–H1A···Cl2^{i}	0.85(3)	2.38(3)	3.209(3)	165(3)
N1B–H1B···Cl3^{ii}	0.86(3)	2.39(3)	3.243(3)	174(3)
N1C–H1C···O1^{iii}	0.85(3)	1.96(3)	2.761(5)	157(3)
N1D–H1D···Cl4^{iv}	0.87(3)	2.34(3)	3.204(3)	173(3)
9·0.6H$_2$O				
N1A–H1A···O1^{iii}	0.86(2)	1.95(2)	2.796(4)	171(2)
N1B–H1B···Cl4^{iii}	0.86(3)	2.32(3)	3.170(3)	172(2)
N1C–H1C···Cl5^{v}	0.86(2)	2.25(2)	3.092(3)	165(2)
N1D–H1D···Cl7^{vi}	0.85(2)	2.22(3)	3.042(3)	162(4)
N1E–H1E···Cl4^{iii}	0.86(3)	2.22(3)	3.064(2)	167(3)
N1F–H1F···Cl6^{iii}	0.87(3)	2.27(3)	3.117(3)	165(3)
N1G–H1G···Cl6^{vii}	0.84(2)	2.37(2)	3.189(2)	163(3)
N1H–H1H···Cl5^{iii}	0.86(3)	2.28(3)	3.105(3)	161(2)
N1I–H1I···Cl4^{viii}	0.86(2)	2.24(2)	3.092(3)	176(2)
10·EtOH·CH$_2$Cl$_2$·H$_2$O				
N1A–H1A···O10^{ix}	0.86(4)	2.04(5)	2.885(6)	169(4)
N1B–H1B···O4^{x}	0.86(3)	2.04(4)	2.877(6)	168(6)
N1C–H1C···O10^{xi}	0.85(5)	2.00(5)	2.826(5)	165(4)
N1D–H1D···O9^{vii}	0.86(5)	1.90(5)	2.747(6)	172(6)
O9–H9···O5^{xii}	0.82(6)	2.02(6)	2.797(5)	159(7)
O10–H101···O3^{iii}	0.83(3)	1.98(3)	2.806(6)	177(8)
O10–H102···O6^{iii}	0.83(5)	2.04(5)	2.850(6)	164(5)
11·MeCN				
N1A–H1A···O3^{xiii}	0.85(3)	2.16(3)	2.980(3)	163(3)
N1B–H1B···O3^{xiv}	0.84(2)	2.09(2)	2.914(3)	169(3)

[a] Symmetry codes: (i) 3/2-x, y, -1/2+z; (ii) 1+x, y, z; (iii) x, y, z; (iv) x, 3/2-y, 1/2+z; (v) 2-x, 2-y, 1-z; (vi) x, 1+y, z; (vii) 1+x, y, -1+z; (viii) 2-x, 1-y, 1-z; (ix) -1+x, y, z; (x) -1+x, 1-y, -1/2+z; (xi) -1+x, 1+y, z; (xii) -1/2+x, -1/2+y, z; (xiii) 1-x, -1/2+y, 1/2-z; (xiv) 1-x, 2-y, 1-z.

The composition of this compound is totally different compared to that of **8**, but its 3D assembly is organized by the same hydrogen-bonding motif: namely, the encapsulated chloride counterions interlink the surrounding A, B and C $[CuCl(HL')_3]^+$ cations *via* multiple (up to four) N–H···Cl$_{counterion}$ interactions (Fig. 4). This is realized either through the individual Cl4 and Cl6 counterions or the bulkier Cl5/O1/Cl7 counterion/solvent clusters. It is noteworthy, probably for steric reasons, that the A, B and C species are not directly linked to each other as in compound **8**; instead, their coordinated chlorides can only form multiple weak C–H···Cl contacts with neighbouring cations. Despite the large number of aromatic rings present, only two intermolecular π···π and some weak C–H···π contacts have been detected, probably due to the separating action of the intervening chloride ions. It is again evident that coordination geometry, conformational flexibility of the ligands, and freedom of molecular orientation (thanks to $Z' = 3$) are the main parameters of the system which, through the appropriate space group, effectively contribute to the formation of the maximum possible number of the hierarchically prevailing N–H···Cl synthons.

Description of the structures of complexes 3–6, 7 and 10

The $[CuL_4]X_2$·solvent type complexes with X = NO_3^- (**3**) or ClO_4^- (**4**, **5**, **6**) have as a common feature the charged $[CuL_4]^{2+}$ group, in which Cu^{II} is coordinated through the pyridine-type nitrogen donor atom from each of the four ligands; this results in a slightly distorted CuN_4 square planar geometry with τ_4 parameter values of 0.03 (**3**), 0.06 (**4**), 0.06 (**5**) and 0.08 (**6**). Compound **3** was prepared in the presence of both Cl^- and NO_3^- ions, but it seems that the Cu:L ratio (1:2.5) eventually favoured the formation of the $[CuL_4]^{2+}$ group utilizing the nitrates as counterions. On the other part, we decided to use the weakly-coordinating perchlorate ion with a series of different solvents (complexes **4**, **5**, **6** and **10**) aiming at possible interesting changes in the structure of the products; it is evident that the $[CuL_4]^{2+}$ cation has prevailed in all instances (Fig. 5). In a manner similar to that for complexes **8** and **9**, the four ligands within each $[Cu(ligand)_4]^{2+}$ cation are associated in pairs *via* two intramolecular π···π stackings, resulting in a total of four contacts and ensuring rigidity to the cation. As a consequence, the conformation of the $[CuL_4]^{2+}$ groups is similar, the largest differences, possibly due to steric requirements, located in the phenyl rings not participating in these π···π contacts. The overlay

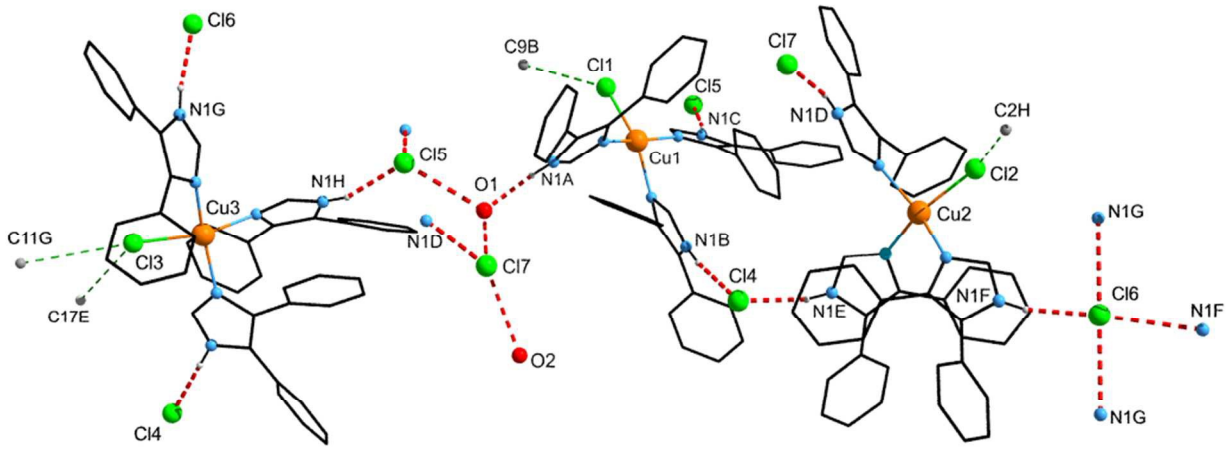

Fig. 4 Part of the structure of compound **9**. The encapsulated chloride ions form multiple strong N–H···Cl interactions with the NH groups of the three crystallographically independent $[CuCl(HL')_3]^+$ cations (with Cu1, Cu2 and Cu3 centres) directing the self-assembly process. Only contact H-atoms are drawn.

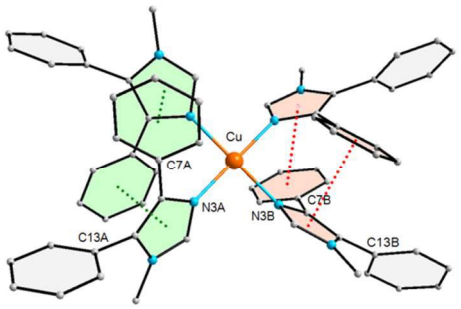

Fig. 5 The $[CuL_4]^{2+}$ cation of compound **3** with the four intramolecular π···π stackings: $d_{\pi\cdots\pi}$ = 3.665(2) Å, centroid offset = 1.206(6) Å for the green pairs; $d_{\pi\cdots\pi}$ = 3.545(2) Å, centroid offset = 1.296(7) Å for the pink pairs. H-atoms have been omitted.

rmsd values for the $[CuL_4]^{2+}$ groups (**3** being the reference one) are 0.356 Å (**3**–**4**), 0.376 Å (**3**–**5**) and 0.465 Å (**3**–**6**). The asymmetric unit of compound **3** contains half a cation (Z' = ½), the other half generated by a C_2 axis lying on the CuN_4 plane and passing through the metal centre.

The NO_3^- (**3**) and ClO_4^- (**4**–**6**) counterions play the major role in the supramolecular 3D organization of the complexes; through their oxygen atoms, acting as multihydrogen-bonded acceptors, they link neighbouring $[CuL_4]^{2+}$ groups by means of C–H···O contacts (Fig. 6). Some additional contacts formed by the solvents together with weak C–H···π interactions complete the packing of the complexes. The absence of intermolecular π···π interactions in the structures of **3**–**6** (and **10**, *vide infra*), notwithstanding the availability of aromatic rings, could be attributed to the buffering action of the intervening counterions and the 'stiffness' of the $[CuL_4]^{2+}$ groups (owing to the four intramolecular π···π contacts). There is only one such contact (in complex **4**) between two inversion-related rings; however, their centroid-centroid distance of 3.937 Å is longer than the common values (about 3.5 Å) for π···π interactions.

$[Cu_2(OMe)_2(MeOH)_2L_4]\cdot 1.5(ClO_4)\cdot 0.5(NO_2)$ (**7**). This compound, crystallized under solvothermal conditions similar to those used for compound **4**, consists of centrosymmetric dinuclear complexes in which two $\{Cu(MeOH)L_2\}^{2+}$ units are connected by two inversion-related μ-methoxo oxygen bridges (Fig. 7). The Cu···Cu separation is 2.982(1) Å. Each Cu^{II} atom is in a distorted square pyramidal environment; two pyridine-type nitrogen donor atoms from the ligands and two μ-methoxo oxygen atoms are placed in the basal positions and a methanol oxygen atom at the elongated apical position. The metal centre lies 0.108(2) Å above the basal plane towards the apical atom. The τ_5 value, describing the geometry of five-coordinate species,[17] is 0.11 [τ_5 equals 0 for square-pyramidal (C_{4v} or 4*mm*) and 1 for trigonal-bipyramidal (D_{3h} or $\bar{6}$m2) geometries]. The *cis* disposition of the ligands in the $\{Cu(OMe)(MeOH)L_2\}$ units favours the formation of two intramolecular π···π stackings in each unit. As expected, the perchlorates (in a 75:25 substitutional disorder with nitrite counterions) effectively organize the 3D hydrogen-bonding pattern through strong O_{MeOH}–H···$O_{perchlorate}$

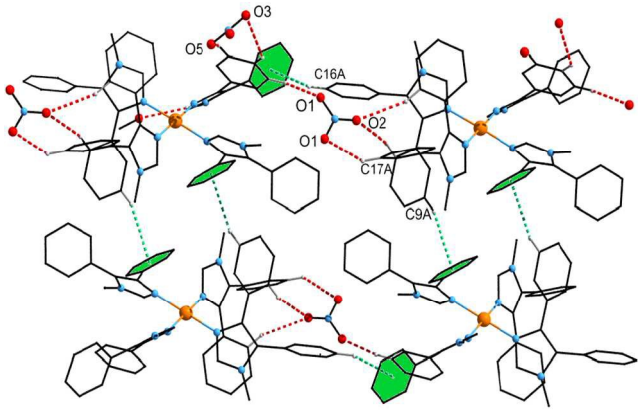

Fig. 6 The incorporated nitrate ions in compound **3** interlink the $[CuL_4]^{2+}$ groups through multiple C–H···O contacts (in red). Some additional weak C–H···π interactions are shown in green. The non-contact H-atoms have been omitted.

and weak C–H···$O_{perchlorate}$ contacts to surrounding ligands (Fig. S2). Two intermolecular π···π interactions per complex and weak C–H···π contacts further interlink the complexes and support the packing.

$[Cu(HL')_4](ClO_4)_2\cdot EtOH\cdot CH_2Cl_2\cdot H_2O$ (**10**·solvent). At the molecular level, the compound resembles complexes **3**–**6**; the charged $[Cu(HL')_4]^{2+}$ group presents a slightly distorted square planar geometry (τ = 0.05) with its four ligands associated in pairs and held tightly *via* π···π stackings. At a glance, it seems that the anticipated N–H···$O_{(ClO_4)}$ interactions would suffice to guide the supramolecular assembly of the structure. However, this requires the $[Cu(HL')_4]^{2+}$ groups to orient themselves within the structure so that their NH groups will face the intervening perchlorates at the right bonding distances and angles, thereby resulting in possible steric hindrance among the involved bulky $[Cu(HL')_4]^{2+}$ groups. In practice, this is effectively addressed by incorporating water and ethanol molecules which form large clusters with the perchlorates, namely $EtOH/ClO_4^-/H_2O/ClO_4^-$, $EtOH/ClO_4^-/H_2O/2(ClO_4^-)$ and $EtOH/ClO_4^-$. In this way, additional binding sites are provided for the NH groups, facilitating the arrangement of the $[Cu(HL')_4]^{2+}$ groups and,

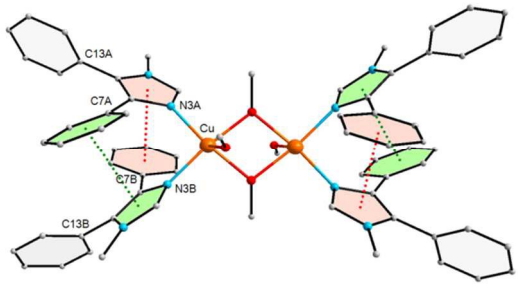

Fig. 7 The structure of the binuclear compound **7** with the four intramolecular π···π stackings: $d_{\pi\cdots\pi}$ = 3.690(3) Å, centroid offset = 0.875(7) for the green pairs; $d_{\pi\cdots\pi}$ = 3.548(2) Å, centroid offset = 0.947(7) for the pink pairs. H-atoms have been omitted.

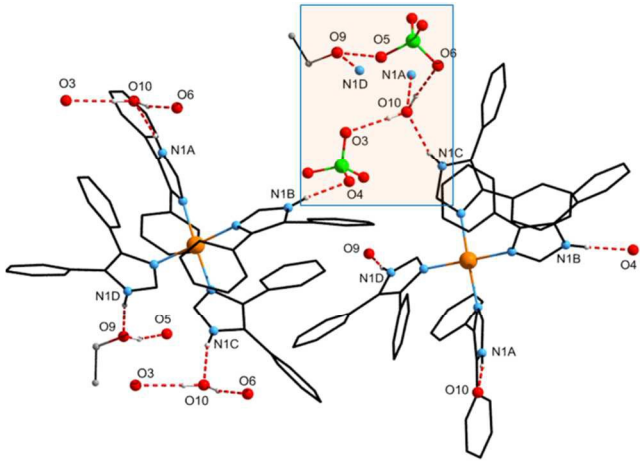

Fig. 8 Perchlorate, water and ethanol solvent molecules form clusters among the bulky $[Cu(HL')_4]^{2+}$ groups in the structure of compound **10** and direct effectively its 3D assembly *via* strong N–H···O(EtOH/ClO_4/H_2O) interactions. Only contact H-atoms are drawn.

ultimately, leading to an effective assembly through strong N–H···O(EtOH/ClO_4/H_2O) interactions (Fig. 8, Table 1). It is interesting that all four water bonding abilities have been exploited –by donating and accepting two hydrogen bonds per water molecule in a tetrahedral environment– justifying its role as a simple and effective tecton.[18-22] The stability of the packing is further enhanced *via* several weak C–H···O(ClO_4) and C–H···Cl(CH_2Cl_2) interactions.

Description of the structure of complex 11

Compound **11** was obtained by replacing the chlorides with nitrates in the reaction system. The metal centre of the complex is in a slightly distorted square-pyramidal N_2O_3 environment (τ_5 = 0.07). The basal plane comprises two imidazole nitrogen atoms and two oxygen atoms of a chelating bidentate nitrate, while the apex of the pyramid is occupied by an oxygen atom of the second

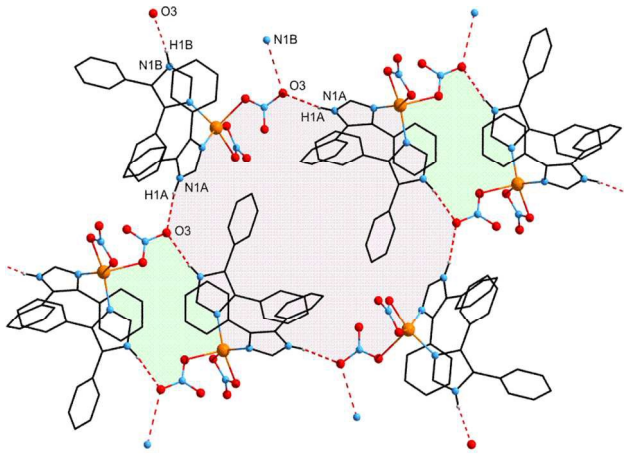

Fig. 9 Part of the structure of compound **11** showing the layer formed by strong N–H···O(NO_3) hydrogen-bonding parallel to the *bc* plane. The resulting $R^4_6(36)$ pattern is shown in light magenta and the $R^2_2(16)$ in green. Only contact H-atoms are drawn.

nitrate coordinated in a monodentate mode[23] (Fig S3). The Cu^{II} centre is displaced out of the basal plane towards the apical oxygen by 0.404(1) Å. As in previous structures, the *cis* disposition of the ligands in the basal plane allows the formation of the intramolecular π···π patterns. Despite the variety of coordinated ions or counterions in the structures of complexes with HL′, the robust N–H···X synthons [X = Cl (**8** and **9**), O(EtOH/ClO_4/H_2O) (**10**) and O(NO_3) (**11**)] are the driving force in all cases (Table 1). At the first level of self-assembly, the molecules of **11** are linked to each other *via* strong N–H···O(NO_3) bonding into layers parallel to the *bc* plane. The resulting centrosymmetric rings, described by $R^2_2(16)$ and $R^4_6(36)$ graph-set motifs,[24] are shown in Fig. 9. The layers are further linked in the third dimension by weak C–H···O(NO_3) interactions towards a 3D supramolecular array. Lastly, small voids in the crystal structure are filled by acetonitrile molecules forming weak C–H···N_{MeCN} contacts without any further significant structural implication.

We note that the bidentate nitrate ion does not participate in any N–H···O contact; it is only the monodentate one that forms such interactions, a single and a bifurcated one, with two neighbouring complexes. The adopted scheme provides an elegant way so as to afford the maximum hydrogen-bonding, taking into consideration the imbalance in donor/acceptor ratio. In parallel, the larger area around the monodentate nitrate –compared with that of the bidentate one– allows the surrounding complexes to adjust themselves more easily to the directionality requirements of the N–H···O synthons. It becomes thus apparent the influence exerted by these packing features on the coordination geometry of the metal centre: 5- *vs* 6-coordinate.

Structural comparisons

In complexes with ligand L (**1**–**7**), the Cu^{II} centres adopt a square planar geometry in the 4-coordinate species **1**–**6** and a square pyramidal coordination in the dinuclear compound **7**. In the absence of strong intermolecular contacts, the packing is primarily based on weak C–H···X interactions, either directly between the complexes as in **1** and **2** (X = Cl or Br) or through the mediation of the intervening NO_3^- (**3**) or ClO_4^- (**4**–**7**) counterions (X = O). Additional C–H···π interactions, together with some C–H···$O_{solvent}$ complex-solvent contacts, strengthen the packing consistency, increasing, in most cases, the dimensionality of the network of interactions. The ability of the coordinated Cl^-/Br^- ions in **1** and **2** to form weak multiple C–H···Cl/Br interactions, sufficient, however, to assemble the molecules in well-organized dense layers without any void space into them, might account for the non-necessity of incorporating any solvent molecules in these structures.

In complexes with ligand HL′, the Cu^{II} centres adopt a seesaw (**8**, **9**) or square planar (**10**) geometry in the 4-coordinate complexes and a square pyramidal coordination in the nitrato species **11**. In-depth analysis of compounds **8**–**11** with ligand HL′ leads to definite conclusions as to the organization of their packing despite the, seemingly, complexity of structures **8** and **9** (with Z′ = 2 and 3, respectively). In all cases, robust N–H···X (X = Cl/O) motifs dominate and direct effectively the supramolecular organization. In this regard, all N–H donor groups of the complexes are involved in synthon formation, either

between independent/symmetry-related molecules or through the Cl^- (**9**) and ClO_4^- (**10**) counterions. When this is sterically unfeasible, as in compound **10** in which the four N–H groups protrude out of the bulky $[Cu(HL')_4]^+$ unit to different directions, appropriately located and oriented solvent water molecules undertake the role to bridge these units through N–H···O_{water} motifs. At a second level of organization, additional but subordinate interactions, such as C–H···Cl/O and C–H···π, complement the self-assembly process. The distortion of the coordination environment (seesaw) of Cu^{II} centres in compounds **8** and **9** could be interpreted as a parameter of flexibility of the system to facilitate and give way to the formation of these structure-directing motifs.

With the exception of the structures of complexes **1** and **2** (having their ligands in *trans* disposition), intramolecular π···π stackings are present in all other complexes (**3**–**11**), a stabilizing pattern encountered in complexes bearing the 4,5-diphenylimidazole moiety . However, at the supramolecular level, this kind of weak interaction, demanding as to the arrangement of the aromatic rings involved, is only present in two crystal packings (**7** and **9**), outlining, in its turn, the emerging hierarchy of interactions in the course of molecular self-assembly.

A comparison of the *molecular structures* of **1**–**11** with those of the previously reported Co(II), Ni(II) and Zn(II) complexes of L and HL′ (Table 2) is useful at this point. The square planar complexes **1**–**6** and **10** have no counterparts in Co(II) and Zn(II) chemistry[6] due to the inability of the latter two metal ions to form square planar complexes. Complexes **1** and **2** are square planar, whereas the corresponding Ni(II) compounds $[NiCl_2L_2]$ and $[NiBr_2L_2]$ have a tetrahedral coordination geometry[6], due to the inability of the $\{X_2+N_2\}$ donor atom combination (X = Cl, Br) to create a strong ligand field around Ni^{II} capable of leading to square planar structures. On the contrary, the $\{Ni^{II}N_4\}^{2+}$ and $\{Cu^{II}N_4\}^{2+}$ (complexes **3**–**6** and **10**) chromophores lead to a square planar coordination for both L and HL′. Complexes $[CoCl_2(HL')_2]$ and $[ZnCl_2(HL')_2]$ have a distorted tetrahedral structure, while the corresponding Cu(II) complex **8** possesses the somewhat related seesaw coordination geometry. Complexes **7** and **11** are unique among the Co(II), Ni(II), Cu(II), Zn(II)/L or HL′ series in having 5-coordinate, square pyramidal geometries. All the above described experimental facts illustrate the $3d^9$ nature of Cu(II), which gives rise to unique electronic effects that affect the molecular geometry (see Introduction). A final point that deserves comment is the dinuclear nature of complex **7**, which reflects the strong tendency of Cu^{II} for spin coupling and formation of dinuclear, polynuclear and polymeric species; in the case of **7** the formation of a dimeric complex is facilitated by the presence of MeO^- groups produced under solvothermal conditions.

Conclusions

At the *supramolecular level*, considering the information reported in Table 2 for all 3d metal complexes of L and HL′ studied, certain interesting conclusions can be drawn: (i) in compounds with the ligand HL′, the robust N–H···X (X = Cl/Br/I/O) pattern is clearly the major factor, the 'handle', that regulates and guides systematically the self-assembly of crystal structures, (ii) in structures without strong patterns (those with L) there occur only weak C–H···X (X = Cl/Br/I/O/N) and C–H···π contacts, available in larger amounts and more evenly distributed around the complexes due to the abundance of the C–H donor groups. It appears that these interactions, individually, act as weak 'hooks'; however, their cumulative effect manages to determine the overall organization of the supramolecular structure. The impact of these interactions in the formation of the crystal packing is reflected in the choice of space group: similar structures (in terms of composition and coordination geometry) formed under the guidance of the same interaction pattern (strong or weak) crystallize in most cases in the same space group. When the latter can no longer support the implementation of the specific interactions together with the geometrical requirements towards an effective close-packed structure,[25] then this is achieved by alternative space groups. Finally, the apparent limited number of intermolecular π···π contacts indicates that these weak and sterically demanding interactions are low in the interaction hierarchy and cannot occur to the detriment of the dominant N–H···X synthons or even of the weak, but numerous, C–H···X interactions.

Experimental

Materials and instruments

Chemicals (reagent grade) were purchased from Merck and Alfa Aesar. All manipulations were performed under aerobic conditions using materials and solvents as received; water was distilled in-house. The ligand 1-methyl-4,5-diphenylimidazole (L) was synthesized as already described in a previous work.[26] Microanalyses (C, H, N) were performed by the University of Patras (Greece) Microanalytical Laboratory. IR spectra were recorded on a Perkin-Elmer PC 16 FT-IR spectrometer with samples prepared as KBr pellets (Fig. S4). *Safety note:* Perchlorate salts are potentially explosive; such compounds should be synthesized and used in small quantities, and treated with great care at all times.

Synthesis of $[CuCl_2L_2]$ (1). A solution of L (0.024 g, 0.10 mmol) and $CuCl_2{\cdot}2H_2O$ (0.013 g, 0.10 mmol) in EtOH/TEOF (20 ml/3 ml) was refluxed for 1 h. The reaction solution was filtered and the resultant green solution was layered with *n*-hexane (40 ml) to produce light green plates of **1** after 1 day; yield *ca*. 60% [based on L]. Anal. Calcd for **1**: C, 63.73; H, 4.68; N, 9.29%. Found: C, 63.64; H, 4.51; N, 9.36%. Selected IR bands (KBr, cm^{-1}): 3448sb, 3056w, 1636w, 1522s, 1484m, 1442m, 1328w, 1196m, 1074w, 826m, 788s, 776s, 736m, 722m, 704s, 692s, 650m.

Synthesis of $[CuBr_2L_2]$ (2). The preparation of **2** was similar to that of **1** except that $CuBr_2$ (0.045 g, 0.20 mmol) was used instead of $CuCl_2{\cdot}2H_2O$. Light green prismatic crystals of **2** were obtained after 5 days in a 30% yield [based on L]. Anal. Calcd for **2**: C, 55.54; H, 4.08; N, 8.09%. Found: C, 55.61; H, 3.89; N, 8.21%. Selected IR bands (KBr, cm^{-1}): 3416sb, 3056w, 1636m, 1616m, 1522s, 1442w, 1376w, 1194m, 1074w, 824w, 788m, 774m, 738w, 722w, 704m, 692m, 648m, 618wb.

Cite this: DOI: 10.1039/c0xx00000x

www.rsc.org/xxxxxx

ARTICLE TYPE

Table 2 Summary of all intra/intermolecular intections present in the crystal structures of the studied copper(II) compounds, together with the analogous complexes of cobalt(II),[6b] zinc(II)[6b] and nickel(II).[6a]

X^-/ ligand	Compound	CG	SG	Weak interactions		Strong interactions	Intra π···π	Inter π···π	Net	Ref.
Cl^-/L	$[CoCl_2L_2]$	T	$P2_1/n$			–	2	–	3D	6*b*
	$[ZnCl_2L_2]$	T	$P2_1/n$			–	2	–	3D	6*b*
	$[NiCl_2L_2]$	T	*Pbcn*			–	2	2	3D	6*a*
	$[CuCl_2L_2]$	SP	$P\bar{1}$			–	–	–	2D	tw
Br^-/L	$[CoBr_2L_2]$	T	$I4_1cd$			–	2	–	3D	6*b*
	$[ZnBr_2L_2]$	T	$I4_1cd$	C–H···X		–	2	–	3D	6*b*
	$[NiBr_2L_2]$	T	$I4_1cd$			–	2	–	3D	6*a*
	$[CuBr_2L_2]$	SP	$P\bar{1}$			–	–	–	2D	tw
I^-/L	$[CoI_2L_2]$	T	$I4_1cd$			–	2	–	3D	6*b*
	$[ZnI_2L_2]$	T	$I4_1cd$			–	2	–	3D	6*b*
Cl^-/HL′	$[CoCl_2(HL')_2]\cdot 2CH_2Cl_2\cdot H_2O$	T	$P\bar{1}$				1	–	3D	6*b*
	$[ZnCl_2(HL')_2]\cdot H_2O$	T	$P\bar{1}$			**N–H···Cl**	1	–	3D	6*b*
	$[CuCl_2(HL')_2]\cdot Me_2CO\cdot 0.25H_2O$	SS	*Pccn*		C–H···π	N–H···O	2	–	3D	tw
	$[CuCl(HL')_3]Cl\cdot 0.6H_2O$	SS	$P\bar{1}$			O–H···Cl	2	2	3D	tw
Br^-/HL′	$[CoBr_2(HL')_2]\cdot CH_2Cl_2$	T	$P2_1/n$	C–H···X			1	–	3D	6*b*
	$[ZnBr_2(HL')_2]\cdot CH_2Cl_2$	T	$P2_1/n$		C–H···Cl	**N–H···Br**	1	–	3D	6*b*
I^-/HL′	$[CoI(HL')_3]I$	T	*I*2/*a*			**N–H···I**	2	2	3D	6*b*
ClO_4^- /L	$[CoL_4](ClO_4)_2\cdot 1.26MeOH\cdot 0.74H_2O$	T	*C*2/*c*			O–H···O	4	–	3D	6*b*
	$[ZnL_4](ClO_4)_2\cdot Me_2CO$	T	$P\bar{1}$			–	3	–	3D	6*b*
	$[NiL_4][NiCl_4]\cdot 2EtOH$	SP	*Aba*2		C–H···Cl	O–H···Cl	4	–	3D	6*a*
	$[NiL_4](OH)_2\cdot H_2O$	SP	*Aba*2			O–H···O	4	–	2D	6*a*
	$[NiL_4]Br_2\cdot 3.4H_2O$	SP	*Aba*2			O–H···Br	4	–	3D	6*a*
	$[NiL_4](NO_3)_2\cdot 2.8MeOH$	SP	$P2_1/n$	C–H···O		O–H···O	4	–	3D	6*a*
	$[NiL_4](ClO_4)_2\cdot Me_2CO$	SP	$Pna2_1$			–	4	–	3D	6*a*
	$[CuL_4](NO_3)_2\cdot 0.6MeOH$	SP	*C*2/*c*		C–H···π	–	4	–	3D	tw
	$[CuL_4](ClO_4)_2\cdot H_2O$	SP	$P\bar{1}$			–	4	–	3D	tw
	$[CuL_4](ClO_4)_2\cdot MeCN\cdot H_2O$	SP	$P\bar{1}$			–	4	–	3D	tw
	$[CuL_4](ClO_4)_2\cdot Me_2CO\cdot 1.6H_2O$	SP	$Pna2_1$			–	4	–	3D	tw
	$[Cu_2(MeO)_2(MeOH)_2L_4](ClO_4)_{1.5}\cdot(NO_2)_{0.5}$	SPY	$P2_1/n$			O–H···O	4	2	3D	tw
ClO_4^- /HL′	$[Co(HL')_4](ClO_4)_2\cdot 1.7Me_2CO\cdot H_2O$	T	$P2_1/c$	C–H···O		**N–H···O** O–H···O	1	–	3D	6*b*
	$[Zn(HL')_4](ClO_4)_2\cdot 2EtOH\cdot 2CHCl_3\cdot H_2O$	T	$P2_1/c$	C–H···O	C–H···π	**N–H···O** O–H···O	1	–	3D	6*b*
	$[Ni(HL')_4][NiCl_2(HL')_2]Cl_2\cdot 1.35H_2O$	SP	$P\bar{1}$	C–H···Cl		**N–H···Cl** N–H···O O–H···Cl	4	2	3D	6*a*
	$[Ni(HL')_4]Br_2\cdot 4.7MeCN$	SP	$P\bar{1}$	C–H···Br	C–H···N C–H··· π	**N–H···Br** N–H···N	4	–	3D	6*a*
	$[Ni(HL')_4]I_2\cdot 2Me_2CO\cdot 0.8H_2O$	SP	*Aba*2	C–H···I	C–H···O	**N–H···I** O–H···I	4	–	3D	6*a*
	$[Ni(HL')_4](NO_3)_2\cdot 2EtOH\cdot 2H_2O$	SP	*Iba*2	C–H···O	C–H···π	**N–H···O** O–H···O	4	–	3D	6*a*
	$[Ni(HL')_4](ClO_4)_2\cdot 2.8Me_2CO$	SP	*Pc*	C–H···O	C–H···π	**N–H···O**	4	–	3D	6*a*
	$[Cu(HL')_4](ClO_4)_2\cdot EtOH\cdot CH_2Cl_2\cdot H_2O$	SP	*Cc*	C–H···O	C–H···Cl	**N–H···O**	4	–	3D	tw
NO_3^- /HL′	$[Co(NO_3)_2(HL')_2]$	T	$P2_1/c$				–	2	3D	6*b*
	$[Zn(NO_3)_2(HL')_2]$	T	$P2_1/c$	C–H···O		**N–H···O**	–	2	3D	6*b*
	$[Cu(NO_3)_2(HL')_2]\cdot MeCN$	SPY	*Pbca*		C–H···N		2	–	3D	tw
NO_2^- /L	$[Co(NO_2)_2L_2]$	O	$I4_1cd$	C–H···O		–	2	–	3D	6*b*
	$[Zn(NO_2)_2L_2]$	O	$I4_1cd$	C–H···N		–	2	–	3D	6*b*
	$[Ni(NO_2)_2L_2]$	O	$P\bar{1}$	C–H···π		–	–	–	2D	6*a*

Compounds of the current work are in bold; supramolecular synthons N–H···X [X = Cl, Br, I or O(ClO_4^- or NO_3^-)] are in bold; CG: coordination geometry; SG: space group; tw: this work; T: tetrahedral; SP: square planar; SS: seesaw; O: octahedral; SPY: square pyramidal.

Cite this: DOI: 10.1039/c0xx00000x

www.rsc.org/xxxxxx

ARTICLE TYPE

Synthesis of $[CuL_4](NO_3)_2\cdot 0.6MeOH$ (3·0.6MeOH). A solution of L (0.175 g, 0.75 mmol), $CuCl_2\cdot 2H_2O$ (0.040 g, 0.30 mmol) and $NaNO_3$ (0.051 g, 0.60 mmol) in MeOH (25 ml) was refluxed for 1 h. The reaction solution was filtered. The resultant green solution was layered with Et_2O (50 ml) to produce pale violet blocks of **3**·0.6MeOH after 32 days; yield *ca*. 10% [based on L]. Anal. Calcd for **3**: C, 68.34; H, 5.02; N, 8.53%. Found: C, 68.16; H, 4.89; N, 8.41%. Selected IR bands (KBr, cm^{-1}): 3054w, 1524m, 1442w, 1382s, 1364s, 1194m, 1074m, 1018m, 980m, 828w, 788m, 774m, 744w, 722w, 698s, 670w, 648m, 616w.

Synthesis of $[CuL_4](ClO_4)_2\cdot H_2O$ (4·H_2O). This compound was synthesized by a solvothermal reaction of L (0.175 g, 0.75 mmol), $NaNO_2$ (0.052 g, 0.75 mmol) and $Cu(ClO_4)_2\cdot 6H_2O$ (0.111 g, 0.30 mmol) in MeOH (8 ml). The resultant solution was heated at 150 °C in a Teflon-lined stainless steel autoclave for 3 days. The reaction system was then slowly cooled (5 °C/h) to room temperature. The reaction solution was filtered. Upon slow evaporation of the filtrate, brown plates of **4**·H_2O were obtained after 2 days in a 60% yield [based on L]. Anal. Calcd for **4**·H_2O: C, 63.13; H, 4.80; N, 9.20%. Found: C, 63.27; H, 4.94; N, 9.31%. Selected IR bands (KBr, cm^{-1}): 3052w, 1522m, 1444w, 1374w, 1198w, 1096s, 1018w, 980w, 846w, 788m, 774sh, 744w, 724w, 700s, 670w, 650m, 622m.

Synthesis of $[CuL_4](ClO_4)_2\cdot MeCN\cdot H_2O$ (5·MeCN·H_2O). A solution of L (0.175 g, 0.75 mmol) and $Cu(ClO_4)_2\cdot 6H_2O$ (0.111 g, 0.30 mmol) in MeCN (25 ml) was stirred for 20 min. The reaction solution was filtered and the resultant green solution was layered with Et_2O (50 ml) to produce brown prismatic crystals of **5**·MeCN·H_2O after 1 day; yield *ca*. 60% [based on L]. Anal. Calcd for **5**·H_2O: C, 63.13; H, 4.80; N, 9.20%. Found: C, 63.28; H, 4.68; N, 9.27%. Selected IR bands (KBr, cm^{-1}): 3378sb, 2900mb, 1654w, 1524w, 1430w, 1374w, 1164m, 1100s, 896w, 788w, 774w, 698w, 650w, 622w.

Synthesis of $[CuL_4](ClO_4)_2\cdot Me_2CO\cdot 1.6H_2O$ (6·Me_2CO·1.6H_2O). A solution of L (0.175 g, 0.75 mmol) and $Cu(ClO_4)_2\cdot 6H_2O$ (0.111 g, 0.30 mmol) in Me_2CO (25 ml) was stirred for 20 min. The reaction solution was filtered. Upon slow evaporation of the filtrate, pale violet prismatic crystals of **6**·Me_2CO·1.6H_2O were obtained after 1 day; yield *ca.* 40% [based on L]. Anal. Calcd for **6**·1.6H_2O: C, 63.07; H, 4.88; N, 9.19%. Found: C, 63.19; H, 4.64; N, 9.31%. Selected IR bands (KBr, cm^{-1}): 3030wb, 1602w, 1524m,, 1422w, 1364w, 1196w, 1094s, 912w, 790m, 774m, 700m, 650w, 624m.

Synthesis of $[Cu_2(OMe)_2(MeOH)_2L_4](ClO_4)_{1.5}(NO_2)_{0.5}$ (7). The preparation of **7** was similar to that of **4**·H_2O except that the quantities of L, $NaNO_2$ and $Cu(ClO_4)_2\cdot 6H_2O$ were 0.059 g, 0.25 mmol/0.017 g, 0.25 mmol/0.037 g, 0.10 mmol, respectively, and the maximum temperature was 120 °C. The total volume of MeOH was the same (8 ml). Blue plates of **7** were obtained after 1 day in a 10% yield [based on copper(II)]. Anal. Calcd for **7**: C, 61.05; H, 5.27; N, 8.38%. Found: C, 61.29; H, 5.48; N, 8.51%. Selected IR bands (KBr, cm^{-1}): 3420sb, 1654m, 1522m, 1444m, 1374w, 1198w, 1098vs, 788m, 744w, 724w, 700s, 650m, 624m.

Synthesis of $[CuCl_2(HL')_2]\cdot Me_2CO\cdot 0.25H_2O$ (8·Me_2CO·0.25H_2O). A solution of HL′ (0.176 g, 0.80 mmol) and $CuCl_2\cdot 2H_2O$ (0.034 g, 0.20 mmol) in Me_2CO (20 ml) was stirred for 30 min. The reaction solution was filtered and the resultant green solution was layered with *n*-hexane (40 ml) to produce brown prismatic crystals of **8**·Me_2CO·0.25H_2O after 5 days; yield *ca.* 30% [based on copper(II)]. Anal. Calcd for **8**·0.25H_2O: C, 62.66; H, 4.21; N, 9.74%. Found: C, 62.52; H, 4.03; N, 9.62%. Selected IR bands (KBr, cm^{-1}): 3148mb, 3068w, 1618w, 1508m, 1458w, 1184w, 1126w, 1074w, 974w, 764s, 722w, 696s, 644m, 618w.

Synthesis of $[CuCl(HL')_3]Cl\cdot 0.6H_2O$ (9·0.6H_2O). A solution of HL′ (0.176 g, 0.80 mmol) and $CuCl_2\cdot 2H_2O$ (0.034 g, 0.20 mmol) in Me_2CO (20 ml) was stirred for 30 min. The reaction solution was filtered. The resultant green solution was layered with *n*-hexane (40 ml) and stored at low temperature (5°C) to produce dark brown prismatic crystals of **9**·0.6H_2O after 14 days; yield *ca*. 40% [based on copper(II)]. Anal. Calcd for **9**·0.6H_2O: C, 67.87; H, 4.68; N, 10.55%. Found: C, 67.71; H, 4.43; N, 10.28%. Selected IR bands (KBr, cm^{-1}): 3142w, 3098w, 1604w, 1588sh, 1510m, 1486m, 1460w, 1442m, 1180w, 1130w, 1072w, 974w, 764s, 722w, 694s, 646m, 616w.

Synthesis of $[Cu(HL')_4](ClO_4)_2\cdot EtOH\cdot CH_2Cl_2\cdot H_2O$ (10·EtOH·CH_2Cl_2·H_2O). A solution of HL′ (0.165 g, 0.75 mmol) and $Cu(ClO_4)_2\cdot 6H_2O$ (0.111 g, 0.30 mmol) in CH_2Cl_2 / EtOH (25ml / 3ml) was refluxed for 1 h. The reaction solution was filtered and layered with pentane (50 ml) to produce brown prismatic crystals of **10**·EtOH·CH_2Cl_2·H_2O after 2 days; yield *ca.* 60% [based on HL′]. Anal. Calcd for **10**·H_2O: C, 62.04; H, 4.34; N, 9.65%. Found: C, 62.28; H, 4.11; N, 9.48%. Selected IR bands (KBr, cm^{-1}): 3146w, 3054w, 1604w, 1526m, 1483m, 1442w, 1194m, 1098vs, 1016m, 789m, 778w, 742m, 694s, 648m, 628s.

Synthesis of $[Cu(NO_3)_2(HL')_2]\cdot MeCN$ (11·MeCN). A solution of HL′ (0.220 g, 1.00 mmol) and $Cu(NO_3)_2\cdot 3H_2O$ (0.097 g, 0.40 mmol) in MeCN (25 ml) was stirred for 20 min. The reaction solution was filtered. Upon slow evaporation of the filtrate, brown prismatic crystals of **11**·MeCN were obtained after 5 days; yield *ca.* 60% [based on copper(II)]. Anal. Calcd for **11**: C, 57.37; H, 3.85; N, 13.38%. Found: C, 57.21; H, 3.67; N, 13.27%. Selected IR bands (KBr, cm^{-1}): 3146w, 3058w, 1604w, 1526s, 1508m, 1488w, 1458w, 1446w, 1396m, 1340s, 1248m, 1190w, 1160w, 1072w, 976w, 766s, 728w, 698s, 644s, 616w.

Cite this: DOI: 10.1039/c0xx00000x

www.rsc.org/xxxxxx

ARTICLE TYPE

Table 3 Crystal data and structure refinement summary for compounds **1–11**

Compound reference	**1**	**2**	**3**·0.6MeOH	**4**·H_2O	**5**·MeCN·H_2O	**6**·Me_2CO·1.6H_2O
Chemical formula	$C_{32}H_{28}Cl_2CuN_4$	$C_{32}H_{28}Br_2CuN_4$	$C_{64}H_{56}CuN_8$·2(NO_3)·0.6(CH_4O)	$C_{64}H_{56}CuN_8$·2(ClO_4)·H_2O	$C_{64}H_{56}CuN_8$·2(ClO_4)·C_2H_3N·H_2O	$C_{64}H_{56}CuN_8$·2(ClO_4)·C_3H_6O·1.6(H_2O)
Formula Mass	603.02	691.94	1143.95	1217.62	1258.68	1286.51
Crystal system	Triclinic	Triclinic	Monoclinic	Triclinic	Triclinic	Orthorhombic
a/Å	5.8941(5)	6.0510(3)	11.1830(3)	11.5340(10)	11.6404(2)	24.1698(3)
b/Å	7.5206(8)	7.5054(4)	29.7328(7)	15.8814(8)	15.8460(4)	11.6310(2)
c/Å	15.7272(10)	15.6246(14)	17.7124(5)	16.7622(14)	17.0057(3)	21.9833(3)
α/°	103.039(8)	102.512(6)	90.00	71.888(6)	70.703(2)	90.00
β/°	96.056(6)	96.500(6)	98.941(3)	87.185(7)	86.718(2)	90.00
γ/°	94.487(7)	94.693(5)	90.00	87.131(6)	88.159(2)	90.00
Unit cell volume/Å^3	671.62(10)	684.14(8)	5817.8(3)	2912.8(4)	2955.40(10)	6179.92(16)
Temperature/K	100(2)	100(2)	100(2)	100(2)	100(2)	100(2)
Space group	$P\bar{1}$	$P\bar{1}$	*C*2/*c*	$P\bar{1}$	$P\bar{1}$	$Pna2_1$
No. of formula units /unit cell, *Z*	1	1	4	2	2	4
Radiation type	MoKα	MoKα	MoKα	MoKα	MoKα	MoKα
Absorption coefficient, *μ*/mm^{-1}	1.042	3.748	0.438	0.533	0.528	0.508
No. of reflections measured	11388	4261	21740	24309	52029	51538
No. of independent reflections	3214	4261	6325	12025	14900	15593
R_{int}	0.0506	0.0000	0.0386	0.0476	0.0260	0.0249
Final R_1 values ($I > 2\sigma(I)$)	0.0341	0.0485	0.0667	0.0504	0.0350	0.0395
Final $wR(F^2)$ values ($I > 2\sigma(I)$)	0.0691	0.1011	0.1961	0.1012	0.0921	0.1036
Final R_1 values (all data)	0.0569	0.0754	0.0853	0.0981	0.0496	0.0488
Final $wR(F^2)$ values (all data)	0.0709	0.1040	0.2058	0.1103	0.0951	0.1063
Goodness of fit on F^2	0.987	0.993	1.035	0.974	1.068	0.994
CCDC number	1407571	1407572	1407573	1407574	1407575	1407576

Compound reference	**7**	**8**·Me_2CO·0.25H_2O	**9**·0.6H_2O	**10**·EtOH·CH_2Cl_2·H_2O	**11**·MeCN
Chemical formula	$C_{68}H_{70}Cu_2N_8O_4$·(ClO_4)$_{1.5}$·(NO_2)$_{0.5}$	$C_{30}H_{24}Cl_2CuN_4$·C_3H_6O·0.25(H_2O)	$C_{45}H_{36}ClCuN_6$·Cl·0.6(H_2O)	$C_{60}H_{48}CuN_8$·2(ClO_4)·CH_2Cl_2·C_2H_6O·H_2O	$C_{30}H_{24}CuN_6O_6$·C_2H_3N
Formula Mass	1362.58	637.55	806.05	1292.51	669.15
Crystal system	Monoclinic	Orthorhombic	Triclinic	Monoclinic	Orthorhombic
a/Å	11.0254(4)	30.1188(8)	16.2205(7)	24.1824(10)	15.4267(6)
b/Å	22.5624(6)	34.4730(7)	17.8175(6)	12.1343(5)	18.0947(7)
c/Å	14.0280(5)	12.5536(3)	26.7171(6)	22.6611(8)	21.1309(7)
α/°	90.00	90.00	73.031(3)	90.00	90.00
β/°	93.327(3)	90.00	84.929(3)	109.241(4)	90.00
γ/°	90.00	90.00	68.555(4)	90.00	90.00
Unit cell volume/Å^3	3483.7(2)	13034.2(5)	6872.6(4)	6278.2(4)	5898.5(4)
Temperature/K	100(2)	100(2)	100(2)	100(2)	100(2)
Space group	$P2_1/n$	*Pccn*	$P\bar{1}$	*Cc*	*Pbca*
No. of formula units /unit cell, *Z*	2	16	6	4	8
Radiation type	MoKα	MoKα	MoKα	MoKα	MoKα
Absorption coefficient, *μ*/mm^{-1}	0.731	0.866	0.630	0.582	0.800
No. of reflections measured	28303	14162	26894	13741	39158
No. of independent reflections	6814	14162	26894	8695	6404
R_{int}	0.0448	0.0000	0.0000	0.0312	0.0890
Final R_1 values ($I > 2\sigma(I)$)	0.0584	0.0535	0.0475	0.0502	0.0464
Final $wR(F^2)$ values ($I > 2\sigma(I)$)	0.1772	0.1283	0.1425	0.1321	0.0964
Final R_1 values (all data)	0.0737	0.0914	0.0655	0.0535	0.0879
Final $wR(F^2)$ values (all data)	0.1846	0.1361	0.1483	0.1361	0.1039
Goodness of fit on F^2	1.076	1.000	0.952	1.048	0.968
CCDC number	1407577	1407578	1407579	1407580	1407581

X-ray Crystallography

Single-crystals covered with paratone-N oil were scooped up in cryo-loops at the end of a copper pin; X-ray diffraction data were collected (ω-scans) on a SuperNova A Agilent Technologies diffractometer under a flow of nitrogen gas at 100(2) K using Mo Kα radiation (λ = 0.7107 Å). Data were collected and processed by the CRYSALIS CCD and RED software,[27] respectively, and the reflection intensities were corrected for absorption by the multiscan method. All structures were solved by direct methods using SIR92[28] and SHELXS-97[29] and refined by full-matrix least-squares on F^2 with SHELXL-97.[30] All non-H atoms were refined anisotropically, and carbon-bound H-atoms were included in the models at calculated positions and allowed to ride on their carrier atoms. Non-routine aspects of structure refinement are as follows: All imidazole H-atoms on the pyrrolic type N1 atom of the HL′-containing compounds, as well as the hydroxyl H-atoms of solvents in compound **10** (EtOH and H_2O) were located in difference Fourier maps and refined isotropically applying soft distance restraints (DFIX). The structure of **2** was refined as a non-merohedral twin (with an 68 : 32 twin components ratio) and that of **6** as a twin by inversion (55 : 45 twin ratio). The crystallization molecules/counterions in **4** and **5** (H_2O), **6** (ClO_4^-), **9** (Cl^-) and **10** (CH_2Cl_2) are disordered and have been modelled over two orientations, while one NO_3^- counterion and the lattice MeOH in **3** show orientational disorder, the former around a center of symmetry and the latter about a two-fold axis. Compound **7** exhibits substitutional disorder of the ClO_4^- and NO_2^- counterions, with site-occupancy factors of 0.75 : 0.25, respectively, as was concluded after competitive and detailed refinement. Two disordered phenyl rings of complex **9** have been modeled over two orientations. The crystal structures of **8** and **9** contain an area of highly disordered solvent (*n*-hexane and water, respectively) which results in smeared-out electron density, making difficult to model reliably the positions and distribution of these solvents. Therefore, the SQUEEZE function of PLATON[31] was used to remove the contribution of the electron density associated with those molecules from the intensity data. Geometric/crystallographic calculations were carried out using PLATON,[31] OLEX2,[32] X-Seed[33] and WINGX[34] packages; molecular/packing graphics were prepared with DIAMOND[35] and MERCURY.[36] Crystallographic data collection and refinement parameters are listed in Table 3.

Acknowledgements

This work was supported by the Research Committee of the University of Patras, Greece (K. Caratheodory program, Grant No. C.585 to VN). AJT thanks the Cyprus Research Promotion Foundation Grant "ΑΝΑΒΑΘΜΙΣΗ/ΠΑΓΙΟ/0308/12" which is co-funded by the Republic of Cyprus and the European Regional Development Fund.

Notes and references

[a] *Department of Chemistry, University of Patras, 26504 Patras, Greece. Tel: +30 2610 962953; E-mail: nastopoulos@chemistry.upatras.gr*
[b] *Department of Chemistry, University of Cyprus, 1678 Nicosia, Cyprus.*
[‡] *Current address: Department of Chemistry, University of Ioannina, 45110 Ioannina, Greece.*

† Electronic Supplementary Information (ESI) available: Figures, tables with hydrogen-bonding geometries and IR spectra. CCDC reference numbers 1407571–1407581. For ESI and crystallographic data in CIF see DOI: 10.1039/b000000x/

1 S. Leininger, B. Olenyuk and P. J. Stang, *Chem. Rev.*, 2000, **100**, 853; M. M. J. Smulders, I. Riddell, C. Browne and J. R. Nitschke, *Chem. Soc. Rev.*, 2013, **42**, 1728; R. Chakrabarty, P. S. Mukherjee and P. J. Stang, *Chem. Rev.*, 2011, **111**, 6810; C. B. Aakeröy, N. R. Champness and C. Janiak, *CrystEngComm*, 2010, **12**, 22.
2 J. E. Beves, B. A. Blight, C. J. Campbell, D. A. Leigh and R. T. McBurney, *Angew. Chem. Int. Ed.*, 2011, **50**, 9260; T. R. Cook, Y. R. Zheng, P. J. Stang, *Chem. Rev.*, 2013, **113**, 734; B. Moulton and M. J. Zaworotko, *Chem. Rev.,* 2001, **101**, 1629; A. J. Blake, N. R. Champness, P. Hubberstey, W. S. Li, M. A. Withersby and M. Schröder, *Coord. Chem. Rev.*, 1999, **183**, 117.
3 G. R. Desiraju, *J. Am. Chem. Soc.*, 2013, **135**, 9952; K. Biradha, C. Y. Su and J. J. Vittal, *Cryst. Growth Des.*, 2011, **11**, 875; J.-M. Lehn, in *Supramolecular Chemistry. Concepts and Perspectives*, Wiley-VCH, Weinheim, 1995; A. D. Burrows, R. W. Harrington, M. F. Mahon and S. J. Teat, *CrystEngComm*, 2005, **7**, 388; G. R. Desiraju and T. Steiner, in *The Weak Hydrogen Bond In Structural Chemistry and Biology*, Oxford University Press/IUCr, 2001; C. Janiak, *Dalton Trans*., 2000, 3885.
4 S. K. Sommer, L. N. Zakharov and M. D. Pluth, *Inorg. Chem.*, 2015, **54**, 1912; G. R. Desiraju, *Acc. Chem. Res*., 1996, **29**, 441; J.-A. van den Berg and K. R. Seddon, *Cryst. Growth Des.*, 2003, **3**, 643; J. W. Steed and J. L. Atwood, in *Supramolecular Chemistry*, Wiley, Chichester, 2009; P. Gamez, G. A. van Albada, I. Mutikainen, U. Turpeinen and J. Reedijk, *Inorg. Chim. Acta*, 2005, **358**, 1975.
5 K. A. Kounavi, C. Papatriantafyllopoulou, A. J. Tasiopoulos, S. P. Perlepes and V. Nastopoulos, *Polyhedron*, 2009, **28**, 3349; K. A. Kounavi, J. Manos, A. J. Tasiopoulos, S. P. Perlepes and V. Nastopoulos, *Bioinorg. Chem. Appl.* 2010, Article ID 178034 (7pp).
6 (*a*) K. A. Kounavi, E. E. Moushi, M. J. Manos, C. Papatriantafyllopoulou, A. J. Tasiopoulos and V. Nastopoulos, *CrystEngComm*, 2012, **14**, 6492; (*b*) K. A. Kounavi, M. J. Manos, E. Moushi, A. A. Kitos, C. Papatriantafyllopoulou, A. J. Tasiopoulos and V. Nastopoulos, *Cryst. Growth Des*., 2012, **12**, 429.
7 F. A. Cotton, G. Wilkinson, C.A. Murillo and M. Bochmann, in *Advanced Inorganic Chemistry*, Wiley, New York, 6th edn.,1999, pp. 865.
8 D. Reinen, *Commemts Inorg. Chem*., 1983, **2**, 227.
9 C. P. Raptopoulou, S. Paschalidou, A. A. Pantazaki, A. Terzis, S. P. Perlepes, T. Lialiaris, E. G. Bakalbassis, J. Mrozinski and D. A. Kyriakidis, *J. Inorg. Biochem.*, 1998, **71**, 15; S. Zanias, G. S. Papaefstathiou, C. P. Raptopoulou, K. T. Papazisis, V. Vala, D. Zambouli, A. H. Kortsaris, D. A. Kyriakidis and T. F. Zafiropoulos, *Bioinorg. Chem. Appl*., 2010, Article ID 168030 (10pp).
10 A. Hadzovic and D. Song, *Organometallics*, 2008, **27**, 1290.
11 X.-J. Yang, F. Drepper, B. Wu, W.-H. Sun, W. Haehnel and C. Janiak, *Dalton Trans.*, 2005, 256; K. Chłopek, E. Bill, T. Weyhermüller and K. Wieghardt, *Inorg. Chem*., 2005, **44**, 7087.
12 Y. Gong, C. Hu, H. Li, W. Pan, X. Niu and Z. Pu, *J. Mol. Struct.*, 2005, **740**, 153.
13 C. Brock and J. Dunitz, *Chem. Mater.* 1994, **6**, 1118; E. Pidcock and W. D. S. Motherwell, *Cryst. Growth Des*., 2004, **4**, 611.
14 L. Yang, D. R. Powell and R. P. Houser, *Dalton Trans*., 2007, 955.
15 M. Nishio, M. Hirota and Y. Umezawa, in *The CH/π Interaction (Evidence, Nature and Consequences)*, Wiley, New York, 1998; T. Ozawa, E. Tsuji, M. Ozawa, C. Handa, H. Mukaiyama, T. Nishimura, S. Kobayashi and K. Okazaki, *Bioorg. Med. Chem*., 2008, **16**, 10311; M. Nishio, Y. Umezawa, K. Honda, S. Tsuboyama and H. Suezawa, *CrystEngComm*, 2009, **11**, 1757; M. Nishio, Y. Umezawa and M. Hirota, *J. Synth. Org. Chem. Jpn.*, 1997, **55**, 2; H. Suezawa, T. Yoshida,Y. Umezawa, S. Tsuboyama and M. Nishio, *Eur. J. Inorg. Chem*., 2002, **12**, 3148.
16 L. Benisvy, A. J. Blake, D. Collison, E.S. Davies, C. D. Garner, E. J. L. McInnes, J. McMaster, G. Whittaker and C. Wilson, *Chem. Commun.* 2001, 1824; L. Benisvy, A. J. Blake, D. Collison, E. S.

Davies, C. D. Garner, E. J. L. McInnes, J. McMaster, G. Whittaker and C. Wilson, *Dalton Trans.,* 2003, 1975.
17 A. W. Addison, T. N. Rao, J. Reedijk, J. van Rijn and G. C. Verschoor, *Dalton Trans*., 1984, 1349.
18 M. S. D. Su and J. D. Wuest, *J. Am. Chem. Soc*., 1991, **113**, 4696.
19 C. H. Görbitz and H. P. Hersleth, *Acta Crystallogr*., 2000, B**56**, 526.
20 S. Varughese and G. R. Desiraju, *Cryst.Growth Des.*, 2010, **10**, 4184.
21 S. J. Jennifer and P. T. Muthiah, *Inorg. Chim. Acta*, 2014, **414**, 170.
22 A. C. Kalita, K. Sharma and R. Murugavel, *CrystEngComm*, 2014, **16**, 51.
23 G. J. Kleywegt, W. G. R. Wiesmeijer, G. J. Van Driel, W. L. Driessen, J. Reedijk and J. H. Noordik, *Dalton Trans*., 1985, 2177.
24 M. C. Etter, *Acc. Chem. Res*. 1990, **23**, 120; J. Bernstein, R. E. Davis, L. Shimoni and N.-L. Chang, *Angew. Chem. Int. Ed.*, 1995, **34**, 1555; J. Grell, J. Bernstein and G. Tinhofer, *Acta Cryst.*, 1999, B**55**, 1030.
25 A. I. Kitaigorodsky, in *Molecular Crystals and Molecules*, Academic Press, New York, 1973.
26 J. McMaster, R. L. Beddoes, D. Collison, D. R. Eardley, M. Helliwell, and C. D. Garner, *Chem.–Eur. J.*, 1996, **2**, 685.
27 *CrysAlis CCD and CrysAlis RED*, Oxford Diffraction Ltd, Abingdon, Oxford, UK, 2009.
28 A. Altomare, G. Cascarano, C. Giacovazzo, A. Guagliardi, M. C. Burla, G. Polidori and M. Camalli, *J. Appl. Crystallogr*., 1994, **27**, 435.
29 G. M. Sheldrick, *SHELXS-97*, *Program for solution of crystal structures*, University of Göttingen, Germany, 1997.
30 G. M. Sheldrick, *SHELXL-97*, *Program for refinement of crystal structures*, University of Göttingen, Germany, 1997.
31 A. L. Spek, *Acta Crystallogr*., 1990, A**46**, C34.
32 O. V. Dolomanov, L. J. Bourhis, R. J. Gildea, J. A. K. Howard and H. Puschmann, *J. Appl. Crystallogr*., 2009, **42**, 339.
33 L. J. Barbour, *J. Supramol. Chem.*, 2001, **1**, 189.
34 L. J. Farrugia, *J. Appl. Crystallogr*., 1999, **32**, 837.
35 K. Brandenburg, *DIAMOND: Program for Crystal and Molecular Structure Visualization*, Crystal Impact GbR, Bonn, Germany, 2011.
36 C. F. Macrae, P. R. Edgington, P. McCabe, E. Pidcock, G. P. Shields, R. Taylor, M. Towler and J. van de Streek, *J. Appl. Crystallogr*., 2006, **39**, 453.

Supramolecular features in the engineering of 3d metal complexes with phenyl-substituted imidazoles as ligands: the case of copper(II)

Konstantina A. Kounavi, Alexandros A. Kitos, Eleni E. Moushi, Manolis J. Manos, Constantina Papatriantafyllopoulou, Anastasios J. Tasiopoulos, Spyros P. Perlepes and Vassilios Nastopoulos

Textual abstract for the Table of contents

Interesting packing features resulting from the interplay of supramolecular interactions and coordination geometries characterize eleven Cu(II) complexes with phenyl-substituted imidazoles.

Graphical abstract for the Table of contents